Preparation of New Electron-Accepting π-Conjugated Polyquinoxalines. Chemical and Electrochemical Reduction, Electrically Conducting Properties, and Use in Light-Emitting Diodes

Takakazu Yamamoto,* Kiyoshi Sugiyama, Takashi Kushida, Tetsuji Inoue, and Takaki Kanbara

Contribution from the Research Laboratory of Resources Utilization, Tokyo Institute of Technology, 4259 Nagatsuta, Midori-ku, Yokohama 226, Japan

Received December 11, 1995[⊗]

Abstract: Dehalogenation polycondensation of 5,8-dibromoquinoxaline derivatives and 2,6-dibromoquinoxaline with zerovalent nickel complex affords a series of π-conjugated polyquinoxalines with a molecular weight of 6×10^3 to 260×10^3. The polymers are electrochemically reduced (or n-doped) with an $E°$ value of -1.75 to -2.35 V *vs* Ag/Ag^+ and converted into electrically conducting materials with a conductivity of 1×10^{-4} to 7×10^{-3} S cm^{-1} by chemical reduction. Poly(quinoxaline-5,8-diyl)s with aromatic substituents give strong fluorescence with emission peaks at 450−520 nm in solutions as well as in cast films. A light-emitting diode (LED), ITO/polymer/Mg(Ag) (polymer = poly(2,3-diphenylquinoxaline-5,8-diyl)), emits blue-green light (λ_{max} at about 500 nm). Introduction of hole-transporting layers such as vacuum-deposited or spin-coated thin layers of poly(thiophene-2,5-diyl), poly(*p*-phenylene), and poly(*N*-vinylcarbazole) between ITO and the light-emitting layer enhances electroluminescence efficiency by about 2 orders of magnitude. Polyquinoxalines have an ionization potential of 5.83 ± 0.11 eV and a band gap of 2.56 ± 0.26 eV.

Introduction

It has recently been found that π-conjugated polymers containing electron-withdrawing imine nitrogen(s) (C═N),[1−5] e.g.

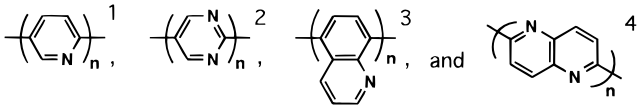

have electron-accepting properties and are susceptible to chemical and electrochemical reduction (or n-doping) to generate a negatively charged carrier in the polymer chain and thus give conducting materials by the reduction. The increase in the number of imine nitrogens enhances the electron-accepting ability of the polymers, and the polymers with two imine nitrogens seem to be more suited for materials to make electric devices using the n-type electrically conducting polymers because of their higher electron-accepting ability.

Among the π-conjugated polymers with two imine nitrogens, poly(quinoxaline-5,8-diyl) derivatives are of particular interest for basic and applied research, since the various dibromo compounds are easily prepared by the reaction in eq 1 and the dibromo compounds can be easily converted into the π-conjugated polymers by dehalogenation polycondensation using nickel complex (eq 2).

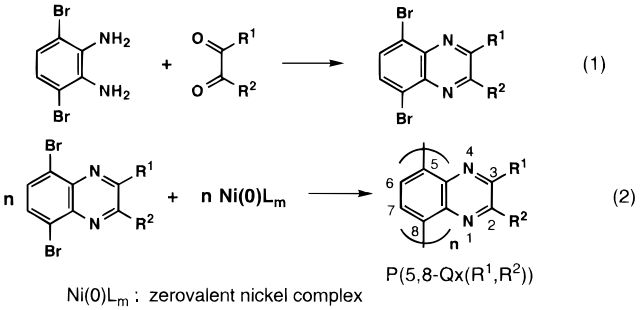

Investigation of chemical and physical properties of the series of the poly(quinoxaline-5,8-diyl) type polymers will make the basic nature of such electron-accepting polymers more clear, and some of the polymers may be useful as materials to construct electric devices.

We here report preparation of such a series of polymers, their chemical, optical, electrical, and electrochemical properties which are controlled by the substituents R^1 and R^2, and application of one of the polymers to light-emitting diodes. Their optical and electrochemical properties are compared with those of another type of polyquinoxaline, poly(quinoxaline-2,6-diyl) (P(2,6-Qx)),[5] which is also prepared by the dehalogenation

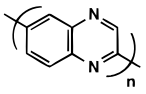

polycondensation using nickel complex. Part of the results have been reported in communications.[5,6]

[⊗] Abstract published in *Advance ACS Abstracts,* April 1, 1996.

(1) (a) Yamamoto, T.; Maruyama, T.; Zhou, Z.-H.; Ito, T.; Fukuda, T.; Yoneda, Y.; Begum, F.; Ikeda, T.; Sasaki, S.; Takezoe, H.; Fukuda, A.; Kubota, K. *J. Am. Chem. Soc.* **1994**, *116*, 4832. (b) Yamamoto, T. *Prog. Polym. Sci.* **1992**, *17*, 1153; *J. Synth. Org. Chem. Jpn.* **1995**, *53*, 999.

(2) Kanbara, T.; Kushida, T.; Saito, N.; Kuwajima, I.; Kubota, K.; Yamamoto, T. *Chem. Lett.* **1992**, 583.

(3) (a) Kanbara, T.; Saito, N.; Yamamoto, T.; Kubota, K. *Macromolecules* **1991**, *24*, 5883. (b) Saito, N.; Kanbara, T.; Nakamura, Y.; Yamamoto, T.; Kubota, K. *Macromolecules* **1994**, *27*, 756.

(4) Saito, N.; Yamamoto, T. *Macromolecules* **1995**, *28*, 4260; *Synth. Met.* **1995**, *69*, 539.

(5) Saito, N.; Kanbara, T.; Kushida, T.; Kubota, K.; Yamamoto, T. *Chem. Lett.* **1993**, 1775.

0002-7863/96/1518-3930$12.00/0

Results and Discussion

Preparation. Dehalogenation polycondensation of dibromoquinoxalines by using the zerovalent nickel complex gives the corresponding polyquinoxalines.

$Ni(0)L_m$: zerovalent nickel complex (a mixture of bis(1,5-cyclooctadiene)-nickel $Ni(cod)_2$ and 2,2'-bipyridine bpy)

Polymers* :

	R^1	R^2		R^1	R^2
P(5,8-Qx) (6.3)	H	H	P(5,8-Qx(diTol)) (24)		
P(5,8-Qx(diEt)) (44)	C_2H_5	C_2H_5	P(5,8-Qx(diAns)) (129)	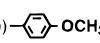	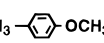
P(5,8-Qx(diHep)) (14)	n-C_7H_{15}	n-C_7H_{15}	P(5,8-Qx(diBP)) (260)		
P(5,8-Qx(MePh)) (33)	CH_3	C_6H_5	P(5,8-Qx(diPy)) (5.8)		
P(5,8-Qx(BuPh)) (9.7)	n-C_4H_9	C_6H_5	P(5,8-Qx(diFu))		
P(5,8-Qx(diPh)) (61)	C_6H_5	C_6H_5			

* $M_w \times 10^{-3}$ determined by a light scattering method is given in parentheses below the code of the polymer (M_w = weight-average moleular weight).

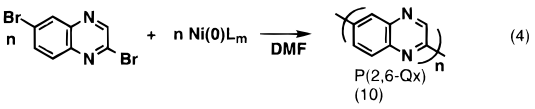

Use of reaction conditions (employment of a mixture of $Ni(cod)_2$ and bpy as $Ni(0)L_m$ in DMF at 60 °C) applied to the previously reported analogous polycondensation[1−4] is also effective in the present polycondensation, and the polymers with high molecular weight are obtained in high yields (88−99%). Data from elemental analysis support formation of the polymers (cf. the Experimental Section and supporting information).

Nonsubstituted P(5,8-Qx) is soluble in CF_3COOH and HCOOH, and insoluble in other organic solvents. Introduction of methyl, ethyl, phenyl, *p*-tolyl, *p*-methoxyphenyl, and 2-furyl substituents does not cause a distinct increase in the solubility, whereas introduction of *p*-phenylphenyl and 2-pyridyl substituents makes the polymers soluble in organic solvents such as halogenated solvents ($CHCl_3$ and $C_2H_4Cl_4$) and NMP. Polymers with long alkyl chains (P(5,8-Qx(diHep))) or an asymmetric structure (P(5,8-Qx(BuPh))) become soluble in various organic solvents. P(5,8-Qx(BuPh)) has the highest solubility, and it shows normal M_z/M_w and M_w/M_n values of 2.1 and 2.2 as determined by the light scattering method and GPC, respectively (M_z = *z*-average molecular weight; M_n = number-average molecular weight).[7] P(5,8-Qx(BuPh)) gives an $[\eta]$ value of 0.95 dL g^{-1} in $CHCl_3$. P(2,6-Qx) is soluble in CF_3COOH and inorganic acids such as concentrated H_2SO_4(aq) and HCl(aq),

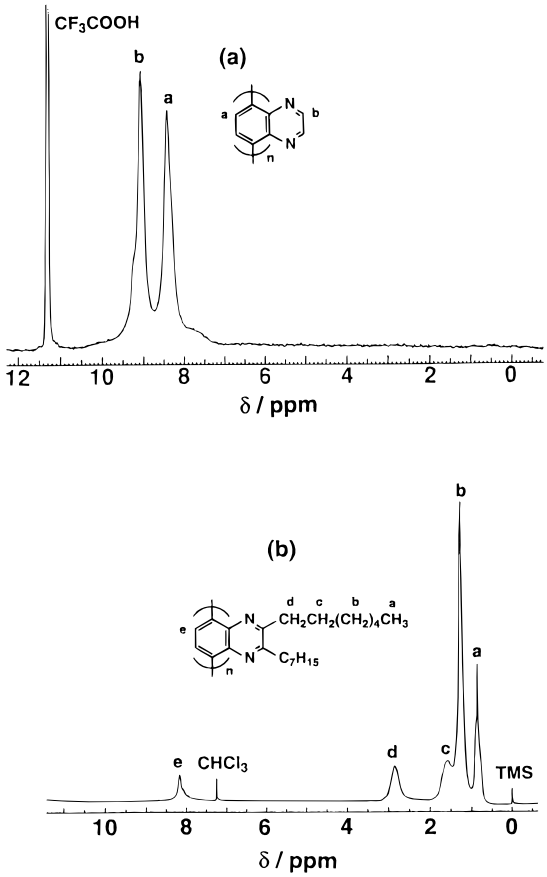

Figure 1. ^{1}H-NMR (100 MHz) spectra of (a) P(5,8-Qx) in CF_3COOD and (b) P(5,8-Qx(diHep)) in $CDCl_3$.

and is partly soluble in HCOOH. The table in the supporting information summarizes the solubility of the polymers in various solvents.

Drying the HCOOH solution of the polymer gives the original polymer as proved by IR spectroscopy, revealing that HCOOH essentially serves as solvent and doeas not form a stable salt with the polymer, as in the case of poly(pyridine-2,5-diyl).[1a] In most cases, drying the CF_3COOH solution also gives solvent-free original polymer; however, in some cases the IR spectrum of the recovered polymer shows a ν(C═O) peak of the solvent or its salt; in the latter case, the recovered polymer is further treated with NH_3(aq) and dried to recover the original polymer.

IR and NMR. IR spectra of the polymers are reasonable for their structures. Absorption peaks of ring vibration (1650−1350 cm^{-1}) and δ(C−H) out-of-plane (1000−650 cm^{-1}) vibrations of the polymers appear at essentially the same positions as those of the corresponding monomers, and ν(C−Br) absorption bands of the monomers are not observable in the IR spectra.

NMR spectra of polyquinoxalines are also reasonable for their structures. Parts a and b of Figure 1 show ^{1}H-NMR spectra of P(5,8-Qx) in CF_3COOD and P(5,8-Qx(diHep)) in $CDCl_3$, respectively. The peaks in the NMR spectra of the polymers are assigned by comparing positions of the peaks with those of quinoxaline and the corresponding monomers. As shown in Figure 1a, P(5,8-Qx) gives two broad peaks of 2,3-H and 6,7-H (peaks b and a in Figure 1a) of the quinoxaline ring at δ 9.1 and 8.4 ppm, respectively. In Figure 1b, a broad peak at δ 8.2 ppm is due to 6,7-H protons of the quinoxaline ring, whereas three broad peaks at about δ 2.9, 1.6, and 1.2 ppm are assigned to the CH_2 protons of the heptyl group, and a peak at δ 0.8 ppm originates from the CH_3 protons of the heptyl group, as depicted in Figure 1b. The peak area ratios agree with the assignment. The ^{1}H-NMR spectrum of P(2,6-Qx) shows broad

(6) (a) Kanbara, T.; Yamamoto, T. *Macromolecules* **1993**, *26*, 3464; (b) Kanbara, T.; Yamamoto, T. *Chem. Lett.* **1993**, 1459. (c) Yamamoto, T.; Inoue, T.; Kanbara, T. *Jpn. J. App. Phys.* **1994**, *33*, L250.

(7) The M_z/M_w value was estimated from the following equation: $M_z/M_w = 1 + 4 \times$ variance. The GPC chart gives the M_w and M_n values of 4.9×10^4 and 2.2×10^4 (polystyrene standard), respectively. The lager M_w value obtained by GPC than that obtained by the light-scattering method may be attributed to a stiffer structure of P(5,8-Qx(BuPh)) than polystyrene. A similar difference between such M_w values has been reported for poly(3-hexylthiophene-2,5-diyl) (Yamamoto, T.; Oguro, D.; Kubota, K. *Macromolecules* **1996**, *29*, 1833). The relatively large $[\eta]$ value of P(5,8-Qx(BuPh)) also supports the stiffer structure. P(5,8-Qx(diBP)) may be partly aggregated in solutions.

Table 1. Optical Data for Polyquinoxalines

polymer	absorption[a] λ_{max}/nm	fluorescnece[b] λ_{max}/nm	excitation[c] λ_{max}/nm	E_g[d]/eV	IP[e]/eV	EA[f]/eV
P(5,8-Qx)	258, 324 (HCOOH)			2.58	5.74	3.16
P(5,8-Qx(diEt))	260, 333 (HCOOH)			2.58	5.72	3.14
P(5,8-Qx(diHep))	258, 330, 374 ($CHCl_3$)	455 ($CHCl_3$)	335	2.82	5.74	2.92
	265, 280, 333 (HCOOH)	460 (film)	335			
P(5,8-Qx(MePh))	330, 385 (NMP)	470 (NMP)	335	2.72		
P(5,8-QxBuPh))	340 (band I), 385 (band II) ($CHCl_3$)	460 ($CHCl_3$)	340	2.70	5.94	3.24
	261, 347 (HCOOH)					
P(5,8-Qx(diPh))	273, 411 (CF_3COOH)	480, 510 ($CHCl_3$)	375, 430	2.48	5.79	3.31
	370, 420 (film)	500 (film)	375, 440			
P(5,8-Qx(diTol))	267, 394 (HCOOH)	480 ($CHCl_3$)	300, 380	2.38	5.74	3.36
		510 (film)	390			
P(5,8-Qx(diAns))	253, 300, 387 ($CHCl_3$)	485 ($CHCl_3$)	310, 395	2.43		
	275, 390 (HCOOH)	505 (film)	330, 395			
P(5,8-Qx(diBP))	264, 310, 384 ($CHCl_3$)	470 ($CHCl_3$)	310, 385	2.70	5.94	3.24
		500 (film)	330, 385			
P(5,8-Qx(diPy))	252, 287, 353 ($CHCl_3$)	520 ($CHCl_3$)	325	2.53		
	308 (HCOOH)	520 (film)	310			
P(5,8-Qx(diFu))	313, 396 (NMP)	500 (NMP)	315, 395	2.53		
P(2,6-Qx)	292, 394 (HCOOH)			2.30		

[a] The solvent or the state of measurement is shown in parentheses. [b] The solvent or the state of measurement is shown in parentheses. [c] Monitored at λ_{max} of the fluorescence. In the same solvent or state indicated by footnote *b*. [d] Band gap estimated from the onset position of the absorption band. [e] Ionization potential estimated from the threshold potential for generation of photoelectrons by irradiation of UV light. [f] Electron affinity estimated from the following equation: $EA = IP - E_g$.

peaks in the range δ 7.5−10.0 ppm due to protons of the quinoxaline ring. P(2,6-Qx) is considered to be constituted of three types of biquinoxaline units, i.e., head-to-tail (2,6-linkage), head-to-head (2,2′-linkage), and tail-to-tail (6,6′-linkage) units. This seems to complicate the ^{1}H-NMR spectrum of P(2,6-Qx). ^{13}C-NMR data of the polymers are also reasonable for their structure and given in the supporting information.

UV−Vis, IP, EA, and Fluorescence. Table 1 indicates UV−vis and fluorescence data of polyquinoxalines as well as data of the ionization potential (IP) and electron affinity (EA) of the polymers. The UV−vis spectrum of a formic acid solution of P(5,8-Qx) exhibits the lowest energy $\pi-\pi^*$ absorption peak at 324 nm. On the other hand, P(2,6-Qx) gives the lowest energy $\pi-\pi^*$ absorption peak at 394 nm in formic acid (the last line in Table 1). The appearance of the $\pi-\pi^*$ absorption band of P(2,6-Qx) at a considerably longer wavelength than that of P(5,8-Qx) is attributed to the presence of a more highly extended π-conjugation system in P(2,6-Qx) than that in P(5,8-Qx), presumably due to less sterically hindered bonding between the monomer units in P(2,6-Qx).[4,5] Other P(5,8-Qx) type polymers with various substituents show the UV−vis absorption peaks near that of P(5,8-Qx), although the $\pi-\pi^*$ absorption peaks of the polymers with aromatic substituent(s) exhibit shifts to longer wavelengths due to formation of larger π-conjugation systems by participation of the aromatic substituents. The band gap (E_g) of the polymers is estimated to be about 2.3−2.8 eV from the optical absorption band.

The polymers have an ionization potential (IP) of about 5.7−5.9 eV as determined from the threshold potential for generation of photoelectrons by irradiation with ultraviolet light. From the IP and E_g valves, the electron affinity (EA) of the polymers is estimated to be about 3.0−3.4 eV. The EA value is larger than those of PPP (EA = 2.1 eV), poly(naphthalene-2,6-diyl) (EA = 2.5 eV), and poly(quinoline-2,6-diyl) (EA = 2.8 eV), which are calculated by a valence effective Hamiltonian method.[8] The EA value is also larger than that of poly(*p*-phenylenevinylene) (PPV, EA = 2.6 eV).[9] These results support the highly electron-accepting properties of polyquinoxalines.

Most of polyquinoxalines without aromatic substituents exhibit only weak fluorescence (or photoluminescence, PL) in solutions as well as in cast films. P(5,8-Qx(diHep)) shows a moderately strong fluorescence with a peak at 455 nm in $CHCl_3$. In contrast to the weak or moderately strong fluorescence of these polymers, polyquinoxalines having aromatic substituent(s) show very strong fluorescence in organic solutions as well as in cast films with a peak at about 460−520 nm, and the fluorescence data are summarized in Table 1. The λ_{max} values of the fluorescence peaks essentially agree with the onset positions of the absorption bands which correspond to the band gap E_g of the polymers, indicating that the fluorescence takes place by migration of electrons in the conduction band to the valence band. The strong fluorescence from the polymers with the aromatic substituent(s) indicates the importance of expansion of the π-conjugation system by introducing the aryl group(s). The fluorescence peak observed with films shows some shift from that observed with solutions, suggesting changes in electronic states of the polymer molecule by interaction with neighboring polymer molecules in the film. However, the degree of the shift is much smaller than that (about 120 nm) observed with a film of poly(pyridine-2,5-diyl),[1a] which was attributed to formation of an excimer-type adduct in the solid state.

In contrast to the strong fluorescence of the polymers with the aryl group(s) in nonacidic solutions as well as in cast films, the original fluorescence is not observable in CF_3COOH or formic acid solutions. Protonation of imine nitrogen(s) of the polymers seems to change the electronic state(s) of the polymer and/or process of the fluorescence. Protonation of P(5,8-Qx-(BuPh)) can be followed by UV−vis spectroscopy. For example, addition of CF_3COOH (1.1×10^{-2} to 4.0×10^{-2} M) to a $CHCl_3$ solution of P(5,8-Qx(BuPh)) leads to a continuous decrease in the intensity of the absorption band at 385 nm (band II in Table 1); at $[CF_3COOH] = 1.7 \times 10^{-2}$ M, the intensity of band II decreases to about half. To the contrary, band I of P(5,8-Qx(BuPh)) at 340 nm (Table 1) receives only a minor effect

(8) (a) Themans, B.; Andre, J. M.; Brédas, J. L. *Solid State Commun.* **1984**, *50*, 1047; *Mol. Cryst. Liq. Cryst.* **1985**, *118*, 121. (b) Brédas, J. L.; Silbey, R.; Boudreaux, D. S.; Chance, R. R. *J. Am. Chem. Soc.* **1983**, *105*, 6555. (c) Brédas, J. L.; Chance. R. R.; Baughman, R. H. *J. Phys. Chem.* **1982**, *76*, 3673. (d) Brédas, J. L.; Chance, R. R.; Silbey, R.; Nicolas, G.; Durand, Ph. *J. Phys. Chem.* **1982**, *77*, 371.

(9) (a) Bradley, D. D. C. *Synth. Met.* **1993**, *54*, 401. (b) Brown, A. R.; Bradley, D. D. C.; Burroughes, J. H.; Friend, R. H.; Greenham, N. C.; Burn, P. L.; Holmes, A. B.; Kraft, A. *Appl. Phys. Lett.* **1992**, *61*, 2793.

Table 2. Redox Potential for n-Doping of Poly(arylene)s

Poly(arylene)	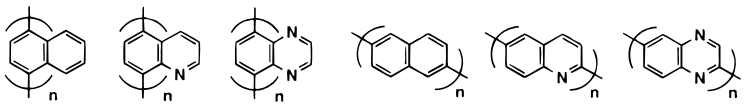					
E°[a] / V	-2.70[b]	-2.37[c]	-1.98	-2.50[b]	-2.11[c]	-1.75

[a] *Versus* Ag/Ag^+. Measured in an acetonitrile solution of $[(C_2H_5)_4N]ClO_4$ (0.1 M). The average of the peak potentials of n-doping and n-undoping is given. [b] From reference 11. [c] From reference 3.

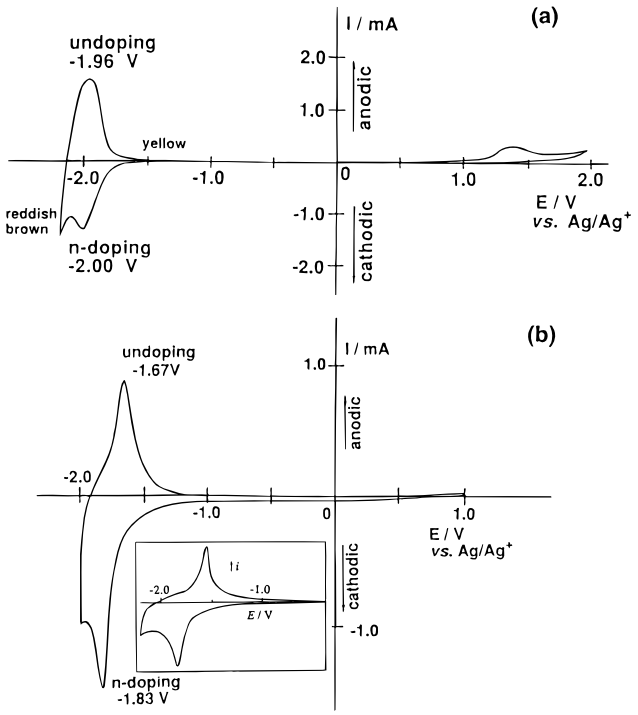

Figure 2. Cyclic voltammograms of films of (a) P(5,8-Qx) and (b) P(2,6-Qx) on platinum plates in an CH_3CN solution of $[(C_2H_5)_4N]ClO_4$ (0.1 M). The sweep rate is 10 mV s^{-1}. Use of a CH_3CN solution of $[(n\text{-}C_4H_9)_4N]ClO_4$ for P(2,6-Qx) gives the CV curve shown in the inset in (b).

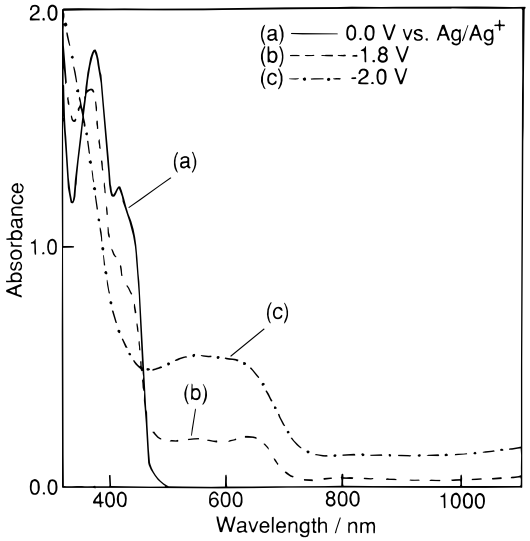

Figure 3. Changes in the absorption spectrum of a film of P(5,8-Qx-(diPh)) on an ITO electrode during electrochemical n-doping in a CH_3-CN solution of $[(C_2H_5)_4N]ClO_4$ (0.1 M).

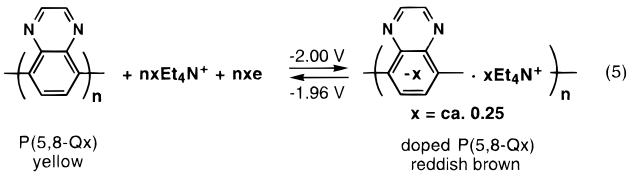

(5)

from added CF_3COOH, revealing that band II is more sensitive to the protonation.[10]

Electrochemical and Chemical Reduction. Parts a and b of Figure 2 exhibit cyclic voltammograms (CVs) of films of P(5,8-Qx) and P(2,6-Qx) cast on a Pt plate. As shown in Figure 2a, P(5,8-Qx) gives rise to an electrochemical active cycle with a reduction (n-doping) peak at −2.00 V *vs* Ag/Ag^+ and a reoxidation (n-undoping) peak of the reduced polymer at −1.96 V *vs* Ag/Ag^+. The reduction and oxidation processes are accompanied by color changes shown in Figure 2a, and the redox reaction can be expressed by eq 5.

The n-doping level (x) is estimated to be about 0.25 from the doping current in Figure 2a. The $E°$ value of the redox reaction estimated from the average of the peak cathode and anode potentials is −1.98 V *vs* Ag/Ag^+, and this value is less negative than those of poly(naphthalene-1,4-diyl) ($E° = -2.70$ V *vs* Ag/Ag^+)[11] and poly(quinoline-5,8-diyl) ($E° = -2.37$ V *vs* Ag/Ag^+)[3] as compared in Table 2. The polymer film is stable for repeated scanning, showing essentially the same CV curve and color change.

The color change of the polymer during the n-doping can be followed spectroscopically with a polymer film cast on an indium/tin oxide glass (ITO), and changes of UV−vis absorption spectrum of P(5,8-Qx(diPh)) during the n-doping are shown in Figure 3. At 0.0 V *vs* Ag/Ag^+ (spectrum a), the nondoped P(5,8-Qx(diPh)) film gives rise to π−π* absorption peaks at 370 and 420 nm and is transparent in a range of 500−1100 nm.

At −1.8 V *vs* Ag/Ag^+ (spectrum b), where the reduction of P(5,8-Qx(diPh)) starts (cf. Table 3), the intensity of the two π−π* absorption bands begins to decrease and a new broad absorption band in a range of 450−700 nm appears. When the polymer film is further reduced at the peak potential, $E = -2.0$ V *vs* Ag/Ag^+, the two π−π* absorption peaks of the nondoped

(10) These results suggest that band II at a longer wavelength mainly originates from π−π* transition along the polymer main chain, and this π−π* transition is strongly affected by the protonation of nitrogen of P(5,8-Qx(BuPh)), which will cause distortion of the bond connecting the monomer units due to an increase in steric repulsion. Assignment of the directions of transition moments of band I and band II is possible by using a stretched poly(vinyl alcohol) (PVA) film[1] containing P(5,8-Qx(BuPh)) molecules, and the results are consistent with the above described assignment of band II; the intensity of band II increases with a stretching ratio[1a] of the PVA film, whereas the intensity of band I receives a minor effect from the stretching ratio.

(11) Tomat, R.; Zecchin, S.; Schiavon, G.; Zotti, G. *J. Electroanal. Chem.* **1988**, *252*, 215.

state become very weak and the new broad absorption band in a range of 450−700 nm becomes stronger. Formation of special electronic states like polaron and bipolaron states accounts for the appearance of the new band. Of the two $\pi-\pi^*$ absorption bands, the one with a longer wavelength seems to receive a stronger effect from the n-doping at −1.8 *vs* Ag/Ag^+.

On the oxidation, the original UV−vis spectrum of the nondoped polymer is obtained, and this doping−undoping cycle can be repeated with good reproducibility. Films of other polyquinoxalines on the ITO electrodes also show similar electrochromic behavior.

In spite of its facile electrochemical reduction (n-doping), the film of P(5,8-Qx) is electrochemically intact against oxidation up to 1.2 V *vs* Ag/Ag^+, where oxidation of electron-donating π-conjugated polymers such as polypyrrole ($E^\circ = -0.3$ V *vs* Ag/Ag^+),[12] polythiophene (0.49 V *vs* Ag/Ag^+),[13] and poly(*p*-phenylene) (ca. 1.1 V *vs* Ag/Ag^+)[13c,14] takes place. All of these data reveal the electron-accepting properties of P(5,8-Qx) due to having two electron-withdrawing imine nitrogens[15] in the recurring unit.

As shown in Figure 2b, P(2,6-Qx) is also electrochemically active only for the reduction (n-doping) and affords a similar CV and color change. The redox potential (E°) of P(2,6-Qx) ($E^\circ = -1.75$ V *vs* Ag/Ag^+) is less negative than that of P(5,8-Qx) ($E^\circ = -1.98$ V) by 0.23 V, and the difference in E° may be explained by a longer effective π-conjugation system of P(2,6-Q) and more direct effect of the electron-withdrawing imine nitrogens in P(2,6-Qx) compared with that of the imine nitrogens in P(5,8-Qx), which exist in the side chain and will not give a direct effect on the π-conjugation system.

The above shown electrochemical data were obtained by using $[(C_2H_5)_4N]ClO_4$ as the electrolyte. Use of $[(n\text{-}C_4H_9)_4N]ClO_4$ in the electrochemical redox reactions of P(5,8-Qx), P(5,8-Qx(diPh)), and P(2,6-Qx) gives essentially the same data, and an example of the CV curves obtained by using $[(n\text{-}C_4H_9)_4N]ClO_4$ is given in an inset in Figure 2b. In this case, scanning can be carried out to a more negative potential, up to −2.3 V *vs* Ag/Ag^+, where flow of irreversible electric current due to decomposition of the solvent starts.

Table 2 compares the E° values of the n-doping of polynaphthylenes,[11] polyquinolines,[3] and polyquinoxalines, all of which have naphthalene-1,4-diyl or naphthalene-2,6-diyl type bonding between the monomer units. As shown in Table 2, introduction of each imine nitrogen makes the n-doping occur more easily with a change in the E° value by about 0.35 V per each of the imine nitrogens, for both types of the polymers.

Other polyquinoxalines are also electrochemically active for the n-doping and n-undoping, and Table 3 summarizes the n-doping and n-undoping potentials as well as electrical conductivity (σ) of sodium-doped polyquinoxalines. As shown in Table 3, the introduction of electron-donating alkyl group(s) into P(5,8-Qx) makes the n-doping more difficult with a shift of the E° value to a more negative side, whereas the introduction of electron-withdrawing aryl group(s) makes the n-doping easier.

Table 3. Electrochemical and Electrical Data of Polyquinoxalines

polymer	peak potential[a]/V: E_{pc} (n-doping)	E_{pa} (n-undoping)	E° [c]	σ[b]/(S cm^{-1}) (Na-doped)
P(5,8-Qx)	−2.00	−1.96	−1.98	1.2×10^{-3}
P(5,8-Qx(diEt))	−2.45	−2.16	−2.31	8.0×10^{-4}
P(5,8-Qx(diHep))	−2.45	−2.25	−2.35	*d*
P(5,8-Qx(MePh))	−2.20	−1.93	−2.07	7.4×10^{-3}
P(5,8-Qx(BuPh))	−2.43	−1.93	−2.18	*d*
P(5,8-Qx(diPh))	−2.02	−1.82	−1.92	1.2×10^{-4}
P(5,8-Qx(diTol))	−1.95	−1.82	−1.89	1.1×10^{-4}
P(5,8-Qx(diAns))	−2.08	−1.87	−1.98	1.1×10^{-4}
P(5,8-Qx(diBP))	−1.98	−1.90	−1.94	4.6×10^{-4}
P(5,8-Qx(diPy))	−2.15	−1.81	−1.98	2.8×10^{-4}
P(5,8-Qx(diFu))	−2.10	−1.98	−2.04	2.8×10^{-3}
P(2,6-Qx)	−1.83	−1.67	−1.75	3.0×10^{-4}

[a] *Versus* Ag/Ag^+. Measured in an acetonitrile solution of $[(C_2H_5)_4N]ClO_4$ (0.1 M) or $[(C_2H_5)_4N]BF_4$ (0.1 M). [b] Treated with sodium naphthalenide. Measured by the two-probe and/or four-probe method. [c] The average of E_{pc} and E_{pa} is given. [d] Not measured due to good solubility in THF.

Nondoped polyquinoxalines are essentially insulators with σ values of less than 10^{-10} S cm^{-1}. Sodium-doped polyquinoxalines have σ values of $10^{-3}-10^{-4}$ S cm^{-1} (measured with compressed powders) as summarized in Table 3. ESR spectra of Na-doped P(5,8-Qx) and P(2,6-Qx) show symmetrical signals at $g = 2.0021$ and 2.0022 with ΔH_{pp} (peak-to-peak width) of 0.31 and 0.26 mT, respectively, at room temperature. Measurement of electrical conductivity of the electrochemically n-doped polymer was not possible. The red-brown or black sodium-doped samples are sensitive to air, and exposure to air caused a rapid decrease in their electrical conductivity with a color change to yellow.

Light-Emitting Diodes. Light-emitting diodes (LEDs) using fluorescent π-conjugated poly(arylene)s such as PPP,[16] PTh and its derivatives,[13c,17] and PPV and its derivatives[9,18] are now actively investigated. Since polyquinoxalines having aromatic substituents show strong fluorescence, the polymers are expected to be useful materials to make LEDs. Actually, ITO/polymer/Mg(Ag) (Figure 4a) simple electric junctions (polymer = P(5,8-Qx(diPh)), P(5,8-Qx(diTol)), P(5,8-Qx(diAns)), P(5,8-Qx(diBP))) emit light on application of an electric field. The peak positions of electroluminescence (EL) spectra of LEDs essentially agree with those of the fluorescence spectra of the polymers (Table 1). However, the intensity of the light from the simple type LEDs is relatively weak; for example, the LEDs using P(5,8-Qx(diPh)) and P(5,8-Qx(diBP)) as the light-emitting materials show emission intensities of 1 cd m^{-2} at 14 V and 10 cd m^{-2} at 18 V, respectively.

(12) Brédas, J. L.; Scott, J. C.; Yakushi, K.; Street, G. B. *Phys. Rev.* **1984**, *B30*, 1023.

(13) (a) Sato, M.; Tanaka, S.; Kaeriyama, K. *Synth. Met*. **1986**, *14*, 279. (b) Zotti, G.; Schiavon, G, *J. Electroanal. Chem.* **1984**, *163*, 385. (c) Yamamoto, T.; Wakayama, H.; Fukuda, T.; Kanbara, T. *J. Phys. Chem.* **1992**, *96*, 8677.

(14) Schiavon, G.; Zecchin, S.; Zotti, G.; Cattarin, S. *J. Electroanal. Chem.* **1986**, *213*, 53.

(15) (a) Baumgärtel, H.; Retzlav, K.-J. *Encyclopedia of Electrochemistry of Elements;* Bard, A. J., Lund, H., Eds.; Marcel Dekker: New York, 1984; Organic Section, Vol. 15, p 168. (b) Newkome, G. R.; Paudler, W. W. *Contemporary Heterocyclic Chemistry*; John Wiley & Sons: New York, 1982.

(16) Grem, G.; Leditzky, G.; Ullrich, B.; Leising, G. *Synth. Met.* **1992**, *51*, 383.

(17) (a) Ohmori, Y.; Uchida, M.; Muro, K.; Yoshino, K. *Jpn. J. Appl. Phys.* **1991**, *30*, L1938; *Solid State Commun.* **1991**, *80*, 605. (b) Greenham, N. C.; Brown, A. R.; Bradley, D. D. C.; Friend, R. H. *Synth. Met.* **1993**, *55*−57, 4134. (c) Berggren, M.; Inganäs, O.; Gustafsson, G.; Rasmusson, J.; Anderson, M. R.; Hjertberg, T.; Wennerström, O. *Nature* **1994**, *372*, 444.

(18) (a) Burroughes, J. H.; Bradley, D. D. C.; Brown, A. R.; Marks, R. N.; MacKay, K.; Friend, R. H.; Burn, P. L.; Holmes, A. B. *Nature* **1990**, *347*, 539. (b) Braun, D.; Hegger, A. J.; Kroemer, H. *J. Electron. Mater.* **1991**, *20*, 945. (c) Vestweber, H.; Greiner, A.; Lemmer, U.; Maht, R. F.; Richert, R.; Heitz, W.; Bässler, H. *Adv. Mater.* **1992**, *4*, 661. (d) Brown, A. R.; Greenham, N. C.; Burroughes, J. H.; Bradley, D. D. C.; Friend, R. H.; Burn, P. L.; Kraft, A.; Holmes, A. B. *Chem. Phys. Lett.* **1992**, *200*, 46. (e) Ueda, M.; Ohmori, Y.; Noguchi, T.; Ohnishi, T.; Yoshino, K. *Jpn. J. Appl. Phys.* **1993**, *32*, L921. (f) Holmes, A. B.; Bradley, D. D. C.; Brown, A. R.; Burn, P. L.; Burroughes, J. H.; Friend, R. H.; Greenham, N. C.; Gymer, R. W.; Halliday, D. A.; Jackson, R. W.; Kraft, A.; Martens, J. H. F.; Pichler, K.; Samuel, I. D. W. *Synth. Met.* **1993**, *55*−57, 4031. (g) Kraft, A.; Burn, P. L.; Holmes, A. B.; Bradley, D. D. C.; Friend, R. H.; Martens, J. H. F. *Synth. Met.* **1993**, *55*−57, 4163. (h) Doi, S.; Kuwabara, M.; Noguchi, T.; Ohnishi, T. *Synth. Met.* **1993**, *55*−57, 4174.

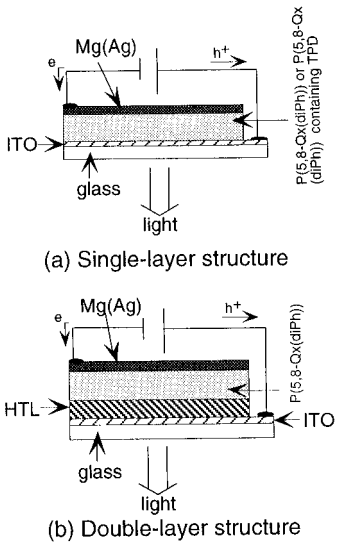

Figure 4. Structures of LEDs: (a) single-layer structure and (b) double-layer structure.

Recently, it has been found that adoption of multilayer type polymer LEDs makes it possible not only to control the color of the emitting light but to improve the emission efficiency.[18d]

Since polyquinoxalines have electron-accepting properties with large EA and IP values, they are considered to serve as good electron-transporting materials. Therefore, introduction of a hole-transporting layer (HTL) between the anode and the polyquinoxaline layer is expected to cause effective injection of holes into the polymer layer, thus making an effective coupling of hole and electron in the polyquinoxaline emitting layer possible to obtain stronger emission of light (Figure 4b).

In order to improve the emission efficiency of LED and to reveal the majority carriers, we have introduced a thin film of vacuum-deposited poly(thiophene-2,5-diyl) (vd-PTh) and poly(*p*-phenylene) (vd-PPP)[1,19] as well as spin-coated poly(*N*-vinylcarbazole) (PVCz) as an HTL between the ITO anode and the polyquinoxaline layer, and examined light-emitting behavior of the following LEDs: ITO/P(5,8-Qx(diPh))/Mg(Ag) (type I); ITO/vd-PTh/P(5,8-Qx(diPh))/Mg(Ag) (type II); ITO/vd-PPP/P(5,8-Qx(diPh))/Mg(Ag) (type III); ITO/PVCz/P(5,8-Qx(diPh))/Mg(Ag) (type IV).

For all LEDs, the forward bias current is obtained when the ITO electrode is biased positively and the Mg(Ag) electrode negatively. Figure 5 shows electric current−potential characteristics of type I and II LEDs. The diodes exhibit good rectification of the electric current, and the forward bias current of the type II LED with the vd-PTh layer drastically increases above 3 V, compared with that of the type I LED without an HTL, indicating that introduction of the vd-PTh layer improves injection of positive charge into the P(5,8-Qx(diPh)) layer. The electric current of type I−IV LEDs exponentially increases with an increase in potential under forward bias conditions. The electric current of type III and IV LEDs is smaller than that of type I and II LEDs, presumably due to the lower hole injection capability of vd-PPP and PVCz layers compared with that of the vd-PTh layer and an increase in the resistivity of the diodes by introduction of the HTLs.

Figure 6 shows EL spectra of type I−IV LEDs. All the EL spectra have a peak at 490 nm, and they essentially agree with the photoluminescence (PL) spectrum of P(5,8-Qx(diPh)) (cf. Table 1), revealing that the EL emission occurs at the P(5,8-Qx(diPh)) layer and emission from HTL is negligible.

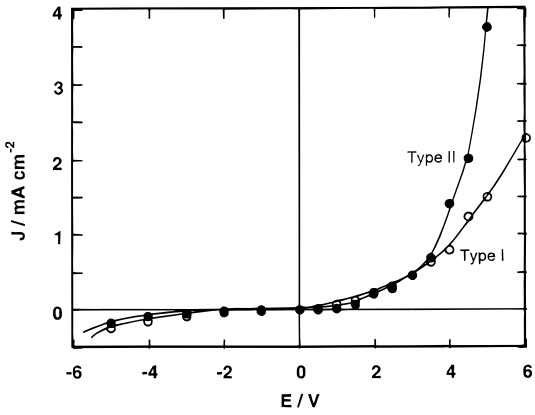

Figure 5. Current density−voltage (J−V) characteristics of the diodes; (a) ITO/P(5,8-Qx(diPh)/Mg(Ag) (type I) and (b) ITO/vd-PTh/P(5,8-Qx(diPh)/Mg(Ag) (type II). The thickness of P(5,8-Qx(diPh)) is about 100 nm. The thickness of vd-PTh is about 50 nm.

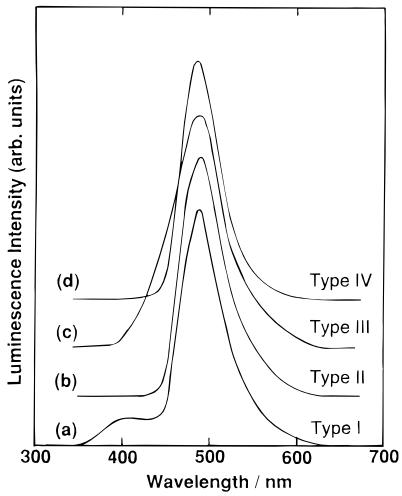

Figure 6. Electroluminescence spectra of LEDs: (a) type I at 11 V, (b) type II at 7 V, (c) type III at 18 V, and (d) type IV at 13 V.

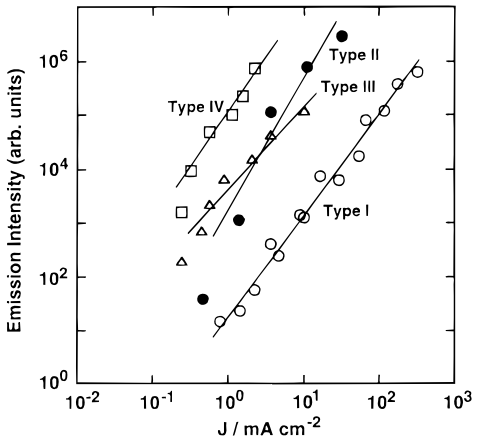

Figure 7. Emission intensity−current density characteristics of LEDs: (a) type I, (b) type II, (g) type III, and (j) type IV electric junctions.

The dependence of the intensity of the emitted light on the injected electric current is shown in Figure 7. The logarithm of the intensity of the emitted light proportionally increases with an increase in the logarithm of the injected electric current, and the emission intensity of type II−IV LEDs with an HTL is much larger than that of the type I LED without an HTL, revealing

(19) (a) Yamamoto, T.; Kanbara, T.; Mori, C. *Synth. Met.* **1990**, *38*, 399. (b) Kanbara, T.; Mori, C.;Wakayama, H.; Fukuda, T.; Zhou, Z.-H.; Maruyama, T.; Osakada, K.; Yamamoto, T. *Solid State Commun.* **1992**, *83*, 771.

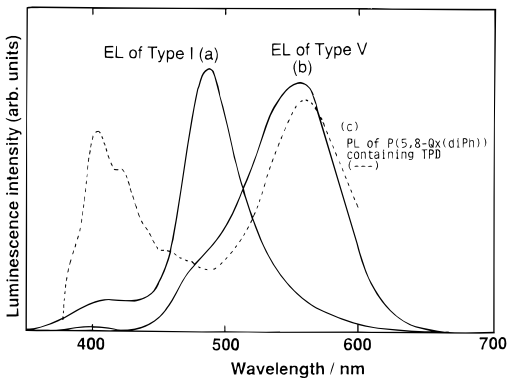

Figure 8. Electroluminescence spectra of (a) type I (at 11 V) and (b) type V (at 6 V) LEDs and (c) photoluminescence spectrum of the spin-casting film of P(5,8-Qx(diPh)) containing TPD (broken line).

that HTLs (vd-PTh, vd-PPP, and PVCz) improve the emission capabilities of the P(5,8-Qx(diPh))-based LED effectively.

PVCz has been used as the hole-transporting material,[20] and p-type semiconducting properties of PTh and PPP have been reported.[13c,21] The results shown in Figures 5 and 7 indicate that the vd-PTh, vd-PPP, and PVCz layers serve as the hole-transporting layer and confine electrons and excitons within the emitting P(5,8-Qx(diPh)) layer. In the case of the type I LED without an HTL, some defect sites may exist at the ITO/P(5,8-Qx(diPh)) interface, and they may allow electrons to move into ITO before recombination with the holes. Type I and II LEDs have emission intensities of 1.0 cd m^{-2} at 14 V and 10 cd m^{-2} at 7 V, respectively.

The type II LED with the vd-PTh layer exhibits a drastic decrease in the emission intensity at a higher voltage (above 8 V), accompanied by an irreversible change in the EL spectrum, which shows a shoulder at about 570 nm (EL peak position of the vd-PTh[13c]). This is considered to be due to migration of the exciton formed in the P(5,8-Qx(diPh)) layer into the vd-PTh layer, and the irreversible change in the EL spectrum suggests a structural change in the vd-PTh/P(5,8-Qx(diPh)) interface under the higher potential conditions.

Addition of *N*,*N*′-diphenyl-*N*,*N*′-bis(3-methylphenyl)[1,1′-biphenyl]-4,4′-diamine (TPD) into the P(5,8-Qx(diPh)) layer in the type I LED (Figure 4a) also leads to an increase in the forward bias current of the single layer type LED, consistent with the hole-transporting properties of TPD,[18g,22] and this LED is referred to as the type V LED. Figure 8 shows a comparison of EL spectra of Type I and V LEDs with and without TPD; Figure 8 also includes a PL spectrum of the spin-cast film of P(5,8-Qx(diPh)) containing TPD. The EL peak position (565 nm) of the type V LED is shifted to a longer wavelength from that of the type I LED by 75 nm, and the EL spectrum essentially agrees with the PL spectrum (Figure 8c) of the film of P(5,8-Qx(diPh)) containing TPD. These results suggest formation of an exciplex or a charge-transfer complex between PQx(diPh) and TPD. The emission intensity of the type V LED is almost the same as that of the type I LED at the same current densities, presumably due to the low emission capability of the exciplex.

The above-described results indicate that P(5,8-Qx(diPh)) serves as a good light-emitting material in LEDs, and effective injection of holes into P(5,8-Qx(diPh)) by selecting a suitable HTL in order to cause an effective coupling of hole and electron in the P(5,8-Qx(diPh)) layer is crucial for development of efficient P(5,8-Qx(diPh))-based LEDs. Addition of a hole-transporting material like TPD is effective for color tuning of the LED, and all these findings will contribute to the design of LEDs using π-conjugated poly(arylene)s.

Conclusion

A series of new π-conjugated polyquinoxalines have been prepared by the organometallic polycondensation. The polymers have strong electron-accepting properties and are easily reduced chemically and electrochemically to give semiconducting materials with color change. The solubility, position of the UV−vis absorption peak, intensity of fluorescence, and electrochemical reduction potential of the polymers are controlled by the substituents in the P(5,8-Qx) type polymer as well as by the mode of connection (at 5,8-positions or 2,6-positions) of the quinoxaline units. Introduction of the aromatic group as the side chain of P(5,8-Qx) gives strongly fluorescent polymers which are useful to make LEDs. Introduction of the hole-transporting layer increases the intensity of light from LEDs, and the results reveal the polymers serve as electron-transporting material.

Experimental Section

Materials. Solvents were dried, distilled, and stored under N_2. Bis(1,5-cyclooctadiene)nickel ($Ni(cod)_2$)[23] and 3,6-dibromo-*o*-phenylenediamine[24] were prepared as reported in the literature. 5,8-Dibromoquinoxaline and its derivatives and 2,6-dibromoquinoxaline were prepared by modifying methods reported by Bird and his co-workers[25] and Sakata and Makino,[26] respectively.

5,8-Dibromoquinoxaline. An aqueous solution (40 wt %, 0.55 g) of glyoxal (3.8 mmol) was added dropwise to 3,6-dibromo-*o*-phenylenediamine (1.0 g, 3.8 mmol) in 25 mL of ethanol. The reaction mixture was refluxed for 3 h. The mixture was cooled, and a pale yellow precipitate was separated by filtration. Recrystallization from acetone gave pale yellow needles (0.75 g, yield 71%). Mp: 226−228 °C dec. Anal. Calcd for $C_8H_4Br_2N_2$: C (33.4), H (1.4), N (9.7), Br (55.5). Found: C (33.4), H (1.3), N (9.5), Br (55.4). IR (KBr, cm^{-1}): 3070, 1575, 1469, 1449, 1371, 1168, 1024, 973, 879, 821, 575, 482. ^1H NMR ($CDCl_3$): δ 8.00 (2H, s, 6,7-H), 9.02 (2H, s, 2,3-H). ^{13}C NMR ($CDCl_3$): δ 123.9, 133.7, 142.8, 146.0. Derivatives of 5,8-dibromoquinoxaline were prepared analogously.

2,6-Dibromoquinoxaline. A mixture of 6-bromo-2-hydroxyquinoxaline[27] (2.74 g, 12.2 mmol), $POCl_3$ (5.25 g, 18.3 mmol), and PBr_3 (10 mL, 0.11 mol) was stirred for 6 h at 170 °C. After cooling to room temperature, the reaction mixture was poured into a mixture of CH_2Cl_2 and ice−water containing $NaHCO_3$, and the product was extracted with CH_2Cl_2. Washing with a saturated aqueous solution of $NaHCO_3$ and a saturated aqueous solution of NaCl in this order, drying with $MgSO_4$, and removal of CH_2Cl_2 by evaporation gave crude 2,6-dibromoquinoxaline. Purification by column chromatography (SiO_2; eluent = 5:95 mixture of $CH_3COOC_2H_5$ and hexane) gave white crystals of 2,6-dibromoquinoxaline (2.26 g, yield 72%) (sublimable). Anal. Calcd for $C_8H_4Br_2N_2$: C (33.4), H (1.4), N (9.7). Found: C (33.7), H (1.4), N (9.5). IR (KBr, cm^{-1}): 3040, 1595, 1535, 1475, 1085, 535.

(20) Shirota, Y.; Kakura, T.; Kanega, H.; Mikawa, H. *J. Chem. Soc., Chem. Commun.* **1985**, 1201.

(21) (a) Tsumura, A.; Koezuka, H.; Anso, T. *Appl. Phys. Lett.* **1986**, *49*, 1210. (b) Dyreklev, P.; Gustafsson, G.; Inganäs, O.; Stubb, H. *Solid State Commun.* **1992**, *82*, 317. (c) Miyauchi, S.; Dei, T.; Tsubata, I.; Sorimachi, Y. *Synth. Met.* **1991**, *41*−43, 1155. (d) Ohmori, Y.; Takahashi, H.; Muro, K.; Uchida, M.; Kawai, T.; Yoshino, K. *Jpn. J. Appl. Phys.* **1991**, *30*, L610. (e) Goldenberg, L. M.; Krinichnyi, V. I.; Nazarovo, I. B. *Synth. Met.* **1991**, *44*, 199.

(22) (a) Tang, C. W.; VanSlyke, S. A. *Appl. Phys. Lett.* **1987**, *51*, 913. (b) Adachi, C.; Tsutsui, T.; Saito, S. *Appl. Phys. Lett.* **1990**, *56*, 799; *57*, 531. (c) Kido, J.; Ohtaki, C.; Hongawa, K.; Okuyama, K.; Nagai, K. *Jpn. J. Appl. Phys.* **1993**, *32*, L917.

(23) Wilke, G. *Angew. Chem.* **1960**, *72*, 581.

(24) Naef, R.; Balli, H. *Helv. Chim. Acta* **1978**, *61*, 2958.

(25) (a) Bird, C. W.; Cheesemaan, W. H.; Sarsfield, A. A. *J. Chem. Soc.* **1953**, 4767. (b) Burton, D. E.; Hughes, D.; Newbold, G. T.; Elvidge, J. A. *J. Chem. Soc. C* **1968**, 1274.

(26) Sakata, G.; Makino, K. *Chem. Lett.* **1984**, 323.

(27) Lumma, W. C., Jr.; Hartman, R. D.; Saari, W. S.; Engelhardt, E. L.; Lotti, V. J.; Stone, C. A. *J. Med. Chem.* **1981**, *24*, 93.

^{1}H NMR($CDCl_3$): δ 7.89 (1H, d, J = 0.49 Hz), 7.89 (1H, d, J = 1.22 Hz), 8.28 (1H, dd, J = 1.22 Hz and 0.49 Hz), 8.85 (1H, br).

Polymerization. P(5,8-Qx). Stirring a mixture of 5,8-dibromoquinoxaline (0.46 g, 1.60 mmol), $Ni(cod)_2$ (0.53 g, 1.90 mmol), 1,5-cyclooctadiene (0.35 mL), and 2,2′-bipyridine (0.30 g, 1.91 mmol) in DMF (25 mL) for 48 h at 60 °C afforded a precipitate of a yellow polymer. The precipitate was collected by filtration, washed with aqueous ammonia, methanol, a warm aqueous solution of ethylenediaminetetraacetic acid (EDTA, pH 3), a warm aqueous solution of EDTA (pH 9), warm distilled water, and warm acetone in this order, and dried under vacuum to obtain a yellow powder of P(5,8-Qx) (yield= 95%). Anal. Calcd for $(C_8\ H_4\ N_2 \cdot H_2O)_n$: C (73.1), H (3.3), N (21.6). Found: C (73.1), H (3.4), N (20.7), Br (0.0). IR (KBr, cm^{-1}): 3026, 1614, 1557, 1489, 1456, 1375, 1334, 1190, 1059, 1024, 964, 867, 498. ^{1}H NMR (CF_3COOD): δ 8.41 (2H, s, 6,7-H), 9.07 (2H, s, 2,3-H). ^{13}C NMR (CF_3COOD): δ 137.3, 139.4, 141.1, 145.9.

Other polyquinoxalines were prepared analogously by using the corresponding dibromoquinoxaline. In the cases of P(5,8-Qx(BuPh)), P(5,8-Qx(diBP)), and P(5,8-Qx(diHep)) further purification was carried out by reprecipitation from $CHCl_3$/acetone.

P(5,8-Qx(BuPh)). Yield: 88%. Anal. Calcd for $(C_{18}H_{16}N_2)_n$: C (83.0), H (6.2), N (10.8). Found: C (82.8), H (5.8), N (10.8), Br (0.0). IR (KBr, cm^{-1}): 3052, 2950−2850, 1550−1330, 694. ^{1}H NMR ($CDCl_3$): δ 0.70 (3H, br, $-CH_3$), 1.22 (2H, br, $-CH_2-$), 1.58 (2H, br, $-CH_2-$), 3.03 (2H, br, $-CH_2-$), 7.3−7.7 (5H, br, −Ph), 8.28 (2H, s, 6,7-H).

P(5,8-Qx(diBP)). Yield: 98%. Anal. Calcd for $(C_{32}H_{20}N_2)_n$: C (88.9), H (4.7), N (6.5). Found: C (88.1), H (4.6), N (6.4), Br (0.0). IR (KBr, cm^{-1}): 3026, 1602, 1485, 1337, 1076, 1007, 980, 842, 765, 732, 694, 522. ^{1}H NMR ($CDCl_3$): δ 7.1−7.8 (18H, m, br, −BPh), 8.49 (2H, s, 6,7-H).

Preparation of LEDs. LEDs consisted of the ITO electrode, the emitting layer of polyquinoxaline, and the Mg(Ag) (Mg:Ag = 10:1) electrode. Thin films of vd-PTh and vd-PPP (about 50 nm) were prepared by vacuum deposition of PTh and PPP onto the ITO electrode,[19] respectively, whereas HTL of PVCz (about 50 nm) was formed by spin-casting from a $CHCl_3$ solution onto the ITO electrode. The light-emitting layers of polyquinoxalines (thickness of about 100 nm) were prepared by spin-casting from a $CHCl_3$ solution onto the ITO or the HTL-coated ITO electrode. P(5,8-Qx(diPh)) had some solubility in $CHCl_3$. When TPD was added to the P(5,8-Qx(diPh)) layer, a $CHCl_3$ solution of a mixture of TPD and P(5,8-Qx(diPh)) (about 1:1 molar ratio between TPD and the monomer unit of P(5,8-Qx(diPh))) was used for the spin-casting. The Mg(Ag) electrode was vacuum deposited onto the emitting layer. The electrode area of the LED was mm 2 × 2 mm.

Acknowledgment. We are grateful to Professor K. Kubota of Gunma University for measurement of the M_z/M_w value. Thanks are due to Messrs. T. Maruyama and B.-L. Lee of our laboratory for experimental support.

Supporting Information Available: Synthetic and analytical data of monomers other than those described in the Experimental Section, analytical data of polymers other than those described in the Experimental Section, experimental details of measurements, and a table showing the solubility of polyquinoxalines (7 pages). This material is contained in many libraries on microfiche, immediately follows this article in the microfilm version of the journal, can be ordered from the ACS, and can be downloaded from the Internet; see any current masthead page for ordering information and Internet access instructions.

JA954173D